

Which Global Moment Tensor Catalog Provides the Most Precise Non-Double-Couple Components?

Boris Rösler^{1,2} , Bruce D. Spencer^{3,4} , and Seth Stein^{4,5}

Abstract

The availability of digital seismic waveform data enabled compilation of seismic moment tensor catalogs that provide information about earthquake source processes beyond what could be derived from earlier methods that assume double-couple sources representing slip on planar faults. This additional versatility involves additional complexity. Moment tensors are determined by inversions minimizing the misfit between observed and synthetic waveforms, and depend on the specifics of the data inverted, the inversion algorithm, and the Earth structure assumed. Hence, substantial uncertainties arise in moment tensors and quantities derived from them, which can be assessed by comparing moment tensors from multiple global and regional catalogs using different data and inversion procedures. While the double-couple (DC) components of moment tensors are generally determined with greater certainty, non-double-couple (NDC) components for the same earthquake sometimes differ significantly between catalogs. This observation raises questions about the reliability of their determination and hence their geological significance. Using the correlation between NDC components in different catalogs, we quantify the reliability of NDC components in moment tensor catalogs through the determination of the effects of unmodeled and inaccurately modeled effects contained in them. We determine that the NDC components in the Global Centroid Moment Tensor catalog are, on average, more precise than in other catalogs, and thus studies on NDC components should be based on this catalog. Furthermore, their uncertainties are largely unrelated to uncertainties in the DC components. Therefore, the reliability of fault angles derived from a moment tensor is largely independent from the reliability of its NDC components.

Cite this article as Rösler, B., B. D. Spencer, and S. Stein (2024). Which Global Moment Tensor Catalog Provides the Most Precise Non-Double-Couple Components? *Seismol. Res. Lett.* **95**, 2444–2451, doi: [10.1785/0220230372](https://doi.org/10.1785/0220230372).

Introduction

Inferring the properties of an earthquake source from the seismic waves it generated is one of seismology's classic inverse problems. The process involves selecting a set of data, assuming a model of the processes by which the source and medium gave rise to the observed data, choosing model parameters, and then solving for a set of source parameters that best matches the model's predictions to the data. The resulting source parameters are often viewed as the best description of the source, and the misfits between the model predictions and data are used to assess how accurately the inferred source parameters describe the actual source.

However, the true uncertainty in describing the source is often substantially greater than the misfit implies. On the one hand, different inversion algorithms may yield different best-fitting solutions. As [Minson *et al.* \(2013\)](#) explain, “there is no unique solution to the inverse problem of determining the rupture history at depth as a function of time and space when

our data are limited to observations at the Earth's surface.” Therefore, a slight change in inversion procedure can lead to different solutions, and thus, “we expect the space of all possible and realistic models to be large” ([Minson *et al.*, 2014](#)). On the other hand, inverting different data types often yields different solutions, so moment tensor solutions may differ for different types of seismic waves used in the inversion. Furthermore, because the model of the processes by which source and medium give rise to the observed data are not fully known, a perfect match between the model predictions and the

1. Earthquake Research Institute, University of Tokyo, Tokyo, Japan,  <https://orcid.org/0000-0001-8596-5650> (BR); 2. Now at Center for Scientific Research and Higher Education at Ensenada (CICESE), Ensenada, Mexico; 3. Department of Statistics, Northwestern University, Evanston, Illinois, U.S.A.,  <https://orcid.org/0000-0001-6155-7249> (BDS); 4. Institute for Policy Research, Northwestern University, Evanston, Illinois, U.S.A.; 5. Department of Earth and Planetary Sciences and Institute for Policy Research, Northwestern University, Evanston, Illinois, U.S.A.

*Corresponding author: boris@eri.u-tokyo.ac.jp

© Seismological Society of America

data may not correctly describe the actual source process. The accuracy of moment tensor inversions is limited by noise from natural and anthropogenic noise in the seismic waveforms (Jechumtálová and Šílený, 2001; Šílený *et al.*, 1996) and sampling limitations due to seismic station coverage (Cesca *et al.*, 2006; Ford *et al.*, 2010; Vera Rodriguez *et al.*, 2011; Domingues *et al.*, 2013). Furthermore, its result depends on the model for elastic and anelastic Earth structure assumed along the path of seismic waves (Cesca *et al.*, 2006; Rößler *et al.*, 2007; Šílený, 2004). Therefore, inversions based on different Earth models may yield different results, and uncertainties remain due to the limitations of the model. Even if the data have no errors and the fault geometry exactly fits them, uncertainties remain due to the limitations of the model because deviations of the structure of the Earth from the model used in the inversion will adjust the moment tensor components to Green's functions generated for an Earth model that does not represent the actual Earth structure along the seismic wave path.

Therefore, determining the geologic meaning of non-double-couple (NDC) components is often difficult. NDC components can arise in three ways. Some appear to be intrinsic, indicating complex source processes differing from slip on a fault for earthquakes in specific geologic environments, notably volcanic areas (e.g., Kanamori and Given, 1982; Ross *et al.*, 1996; Nettles and Ekström, 1998; Shuler, Nettles, and Ekström, 2013; Shuler, Ekström, and Nettles, 2013; Gudmundsson *et al.*, 2016; Rodríguez-Cardozo *et al.*, 2021; Sandanbata *et al.*, 2021). Others are additive, reflecting the combined effect of near-simultaneous rupture on multiple faults with different geometries (e.g., Kawakatsu, 1991; Hayes *et al.*, 2010; Hamling *et al.*, 2017; Scognamiglio *et al.*, 2018; Ruhl *et al.*, 2021; Yang *et al.*, 2021) or a rupture with changes in geometry (Cohee and Beroza, 1994; Wald and Heaton, 1994; Pang *et al.*, 2020). Alternatively, they may be artifactual results of the inversion without geologic meaning. The better determined NDC components are, the more likely they are to represent geological processes. Hence, we explore this issue by assessing the noise in NDC components.

Given these difficulties in determining the source process of an earthquake, we exploit the recent increase in availability of waveform data and improved computer performance and inversion techniques that have enabled the compilation of multiple global and regional moment tensor catalogs with increasingly lower magnitude of catalog completeness. The comparison of multiple catalogs that use different data and inversion procedures offer a way to assess the precision of moment tensors and hence the NDC components contained in them (Rössler *et al.*, 2021, 2023; Rössler and Stein, 2022). This approach finds uncertainties in moment tensors that are much larger than calculated from the misfit between observed and synthetic waveforms and criteria for the reliability of NDC components. Here we use multiple catalogs to quantify the noise contained in the NDC components in each catalog.

Data

The Global Centroid Moment Tensor (Global CMT) Project (Ekström *et al.*, 2012), the U.S. Geological Survey (USGS, Hayes *et al.*, 2009), and the German Research Centre for Geosciences (GFZ) report deviatoric moment tensors for a global distribution of earthquakes derived through inversion procedures that differ in the seismic waveforms used for the inversion in the frequency of the seismic waves inverted and in the inversion algorithm. Their datasets span different times and magnitudes, with the Global CMT catalog being the largest and the longest catalog.

All three catalogs restrict their inversions to have no isotropic components and thus yield deviatoric moment tensors. Their inversion is based on Green's functions generated for preliminary reference Earth model (PREM; Dziewonski and Anderson, 1981)—a 1D Earth model (Hayes *et al.*, 2009; Ekström *et al.*, 2012; Joachim Saul, personal comm., 2022). In an attempt to reduce the uncertainties introduced by lateral heterogeneity in the Earth (Hjörleifsdóttir and Ekström, 2010; Phạm and Tkalčić, 2021; Vasyura-Bathke *et al.*, 2021), several attempts have been made to obtain moment tensor solutions based on Green's functions generated for 3D Earth models for regional earthquakes (Hingee *et al.*, 2011; Hejrani *et al.*, 2017), which, in some cases, were improved using rotational motions (Donner *et al.*, 2020). Sawade *et al.* (2022) compiled the CMT3D moment tensor catalog for global earthquakes with $M_w > 5.5$ using a global 3D Earth model for the inversion.

To compare catalogs, we identify moment tensors describing the same event in different catalogs by similar source times (± 60 s), locations (difference less than 1°), and magnitudes ($M_w \pm 0.5$). We obtain an earthquake's moment magnitude from the scalar moment calculated as the Euclidian norm of the moment tensor (Silver and Jordan, 1982),

$$M_0 = \sqrt{\frac{1}{2} \sum_{i=1}^3 \sum_{j=i}^3 M_{ij}^2}, \quad (1)$$

where M_{ij} represent the six independent moment tensor components, and the factor of 1/2 corrects for double counting the moment associated with the tensors' elements. This yields a dataset of 8222 earthquakes common to the three 1D catalogs with a mean magnitude of M_w 5.6, with 44.7% of earthquakes below magnitude M_w 5.5 (Fig. 1).

Methodology

For each earthquake, the NDC component (the compensated linear vector dipole [CLVD] component in deviatoric moment tensors) is obtained as the ratio of the absolutely smallest and the absolutely largest eigenvalues of the deviatoric moment tensor (Giardini, 1984),

$$\epsilon = \frac{\lambda'_3}{\max(|\lambda'_1|, |\lambda'_2|)}, \quad (2)$$

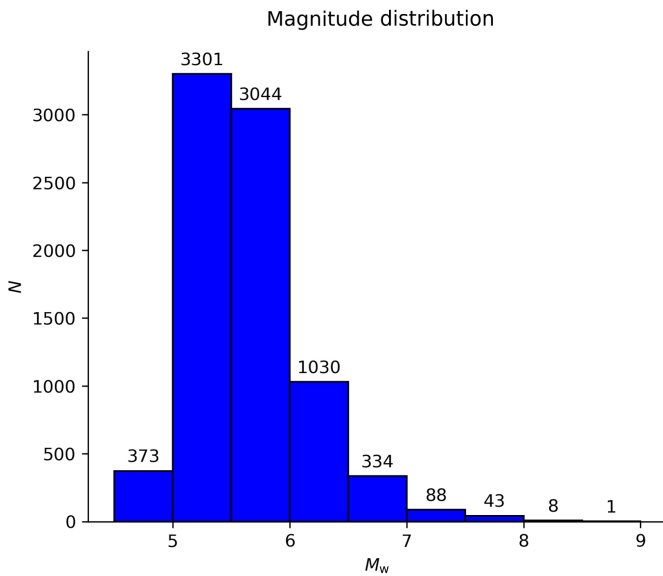


Figure 1. Magnitude distribution of the earthquakes common to the Global Centroid Moment Tensor (Global CMT), U.S. Geological Survey (USGS), German Research Centre for Geosciences (GFZ), and CMT3D catalogs. 20.0% have magnitude below M_w 5.5, and more than half of all earthquakes have magnitude $5.5 \leq M_w \leq 6.0$. The mean and median are M_w 5.8 and 5.7, respectively. The color version of this figure is available only in the electronic edition.

where $\lambda'_1 > \lambda'_3 > \lambda'_2$. For a pure double-couple source corresponding to slip on a planar fault, $\lambda'_3 = 0$ and $\lambda'_1 = -\lambda'_2$. Deviatoric moment tensors found by inversions typically have three nonzero eigenvalues, with $\lambda'_1 \approx -\lambda'_2$ and $|\lambda'_1| \gg |\lambda'_3|$. A negative value of λ'_3 represents a compressional force along the N-axis, whereas a positive λ'_3 represents a dilatational component on the N-axis.

Rösler *et al.* (2021) found that the NDC components for earthquakes common to the Global CMT and USGS catalogs are only weakly correlated—an observation confirmed for earthquakes common to the Global CMT, USGS, and GFZ catalogs by Rösler *et al.* (2023). Apart from the general conclusion that inversions for smaller earthquakes are less reliable and thus more likely to generate spurious NDC components, the correlation of NDC components for earthquakes common to different catalogs can be used to quantify the precision of NDC components in catalogs.

The correlations between pairs of catalogs vary (Fig. 2) for earthquakes common to all three catalogs. NDC components reported by the Global CMT (catalog 1) and USGS (catalog 2) catalogs for the same earthquakes have a correlation coefficient of 0.52, and the correlation between the NDC components in the Global CMT and GFZ (catalog 3) catalogs is 0.47. However, the correlation between the NDC components reported by the USGS and GFZ catalogs is only 0.40. As we show, this difference in correlations suggests varying precision of NDC components between catalogs.

Let ϵ_i denote the true NDC component for earthquake $i = 1, 2, \dots, 8222$. These true NDC components have a distribution S with standard deviation σ_s . The reported NDC components d_{ik} in each catalog k contain random noise that we denote n_{ik} , in which $k = 1, 2, 3$, corresponding to the Global CMT, USGS, and GFZ catalogs, respectively. In the absence of evidence to the contrary and to get insight into the random noise, we assume that the n_{ik} are independent of the true NDC components ϵ_i , and that the reported NDC components d_{ik} in each catalog are the sum of the true NDC components ϵ_i and random noise n_{ik} that represents the combination of all unmodeled and inaccurately modeled effects (e.g., Earth structure),

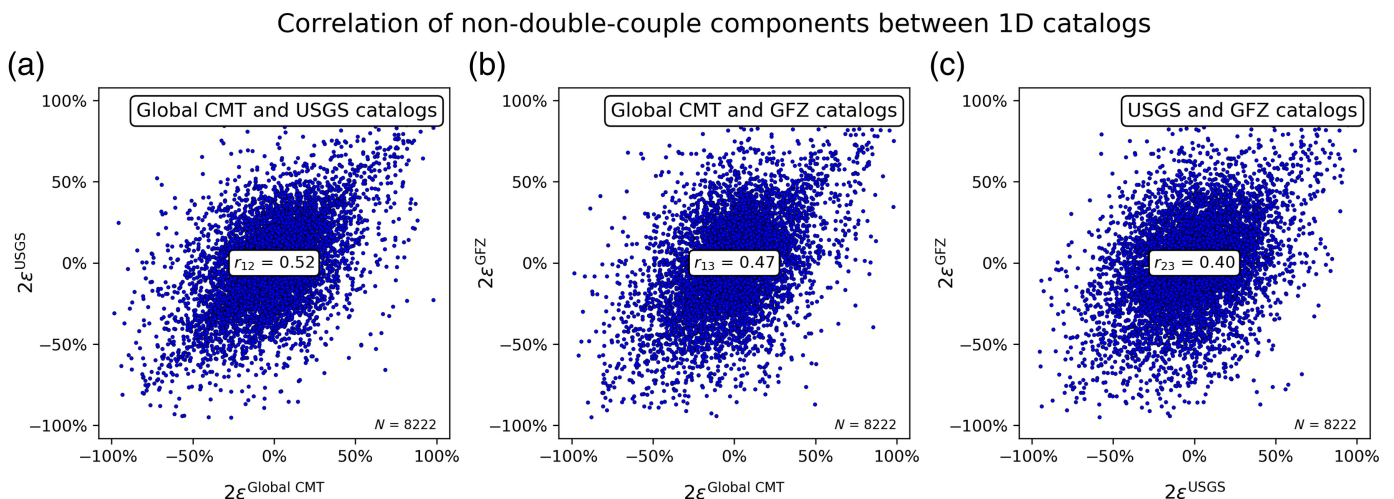


Figure 2. (a–c) Correlation of non-double-couple (NDC) components for the same earthquakes between pairs of catalogs. Correlations that include the NDC components in the Global

CMT catalog are stronger than the correlation between the NDC components in the USGS and GFZ catalogs. The color version of this figure is available only in the electronic edition.

$$d_{ik} = \epsilon_i + n_{ik}. \quad (3)$$

The independence condition implies that the variance of the reported NDC components in each catalog is

$$\sigma_{d_k}^2 = \sigma_s^2 + \sigma_{n_k}^2, \quad (4)$$

where $\sigma_{n_k}^2$ is the variance of the noise in each catalog's NDC components. The standard deviations of the reported measurements for the Global CMT, USGS, and GFZ catalogs are 24.6%, 25.6%, and 27.2%, respectively. It follows from equation (4) that the difference in noise variances for a pair of catalogs A and B is equal to the difference in the variances of their reported measurements,

$$\sigma_{n_A}^2 - \sigma_{n_B}^2 = \sigma_{d_A}^2 - \sigma_{d_B}^2. \quad (5)$$

The noise variances for the USGS and GFZ catalogs are both larger than for the Global CMT catalog, and the Global CMT catalog is thus the most precise. Precision does not take into account systematic error, but the three catalogs have similar means ($\mu_1 = -0.61\%$, $\mu_2 = -0.81\%$, and $\mu_3 = -0.76\%$), and we do not see evidence that they have appreciably different biases, if any.

The standard deviation of the noise is smaller than the standard deviation of the reported measurements, because

$$\sigma_{n_k} = \sqrt{\sigma_{d_k}^2 - \sigma_s^2}. \quad (6)$$

We observe σ_{d_k} , but need to infer σ_s . To do so, we consider two catalogs, catalog A and catalog B . The correlation r_{AB} between the reported NDC components is defined as

$$r_{AB} = \frac{\text{Cov}(d_A, d_B)}{\sigma_{d_A} \sigma_{d_B}}. \quad (7)$$

Using that

$$\begin{aligned} \text{Cov}(d_A, d_B) &= \text{Cov}(\epsilon + n_A, \epsilon + n_B) = \text{Cov}(\epsilon, \epsilon) + \text{Cov}(n_A, n_B) \\ &= \sigma_s^2 + \text{Cov}(n_A, n_B), \end{aligned}$$

the correlation coefficient r_{AB} can be expressed as

$$r_{AB} = \frac{\sigma_s^2 + \text{Cov}(n_A, n_B)}{\sigma_{d_A} \sigma_{d_B}}, \quad (8)$$

and thus the variance of the true NDC components, σ_s^2 , satisfies the relationship

$$\sigma_s^2 = r_{AB} \sigma_{d_A} \sigma_{d_B} - \text{Cov}(n_A, n_B). \quad (9)$$

Correlation between the noise in NDC components of different catalogs could arise from similarities between inversion

procedures or from similarities in the uncertainty of the Earth structure and are thus expected to be zero or positive, in which case $\text{Cov}(n_A, n_B) \geq 0$. However, quantifying the similarity of inversion procedures is difficult due to a lack of documentation of the methods (Rösler *et al.*, 2022) and a lack of error estimation (Duputel *et al.*, 2012), so a precise estimate of the covariance cannot be obtained. We use

$$\hat{\sigma}_s^2 = r_{AB} \sigma_{d_A} \sigma_{d_B} \quad (10)$$

to estimate σ_s^2 based on the empirical evaluation of the correlation coefficient and the data variances from a given set of two catalogs. Using equation (6) we estimate σ_{n_k} by

$$\hat{\sigma}_{n_k} = \sqrt{\sigma_{d_k}^2 - \hat{\sigma}_s^2}. \quad (11)$$

The expected value of $\hat{\sigma}_s^2$ or $E(\hat{\sigma}_s^2)$ is approximately $r_{AB} \sigma_{d_A} \sigma_{d_B}$. The bias in $\hat{\sigma}_{n_k}^2$ is defined as $E(\hat{\sigma}_{n_k}^2) - \sigma_{n_k}^2$ and is approximately equal to $\text{Cov}(n_A, n_B)$. Because $\text{Cov}(n_A, n_B) \geq 0$, the bias is nonnegative, and hence $\hat{\sigma}_s^2$ is estimating an upper bound for σ_s^2 , and $\hat{\sigma}_{n_k}^2$ is estimating a lower bound for $\sigma_{n_k}^2$. The estimate $\hat{\sigma}_s^2 / \hat{\sigma}_{n_k}^2$ of the signal-to-noise ratio (SNR) will therefore be optimistic.

Results

The estimated correlation between catalogs 2 and 3 (0.40) is significantly smaller than between 1 and 2 and between 1 and 3 (0.52 and 0.47, respectively). We use the bootstrap method (Efron, 1979) to determine a confidence interval for the correlation coefficients between NDC components in different catalogs and for the standard deviation of the true NDC components. We randomly draw 8222 earthquakes from our dataset with duplicates allowed. We then calculate the correlation coefficients between the NDC components in each catalog for these earthquakes and repeat the process 10,000 times. This distribution provides the 95% confidence interval for the correlation coefficients as $r_{12} = 0.52 \pm 0.02$, $r_{13} = 0.47 \pm 0.02$, and $r_{23} = 0.40 \pm 0.03$.

The standard deviation of the true NDC components, σ_s , can be estimated from each of the correlation coefficients and the standard deviations of the reported NDC components in the respective catalogs through equation (10). From the correlation between the NDC components in the Global CMT and USGS catalogs and in the Global CMT and GFZ catalogs, σ_s is obtained as $18.1\% \pm 0.4\%$ and $17.7\% \pm 0.4\%$, respectively. However, the correlation between the NDC components in the USGS and GFZ catalogs gives an estimate for σ_s of $16.6\% \pm 0.5\%$, which does not overlap with the confidence interval derived from the other two correlations (Fig. 3a). We therefore conclude that the inversion procedures of the USGS and GFZ catalogs are more similar to each other than to Global CMT, and that

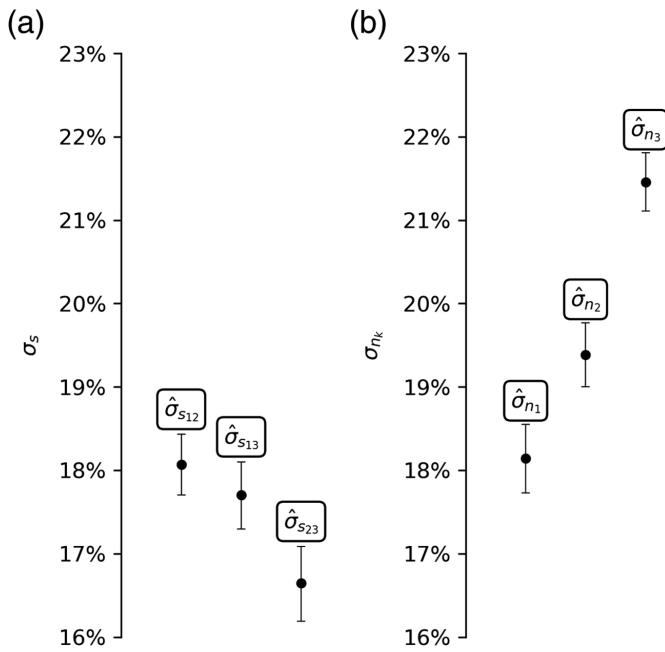


Figure 3. (a) Bootstrap estimates of the mean and 95% confidence intervals for the standard deviation of the true NDC components, σ_s , derived from the different correlations between catalogs between the 2.5th and 97.5th percentile of the distribution of correlation coefficients. The correlation of NDC components in the Global CMT and USGS catalogs (r_{12}) and in the Global CMT and GFZ catalogs (r_{13}) yield consistent estimates for σ_s . However, the confidence interval for σ_s derived from the correlation of NDC components in the USGS and GFZ catalogs (r_{23}) does not overlap with the confidence interval obtained from the other two correlations. (b) Standard deviations of the noise in the NDC components in each moment tensor catalog with their 95% confidence intervals as derived from $\hat{\sigma}_{s_{23}}$. The Global CMT catalog ($\hat{\sigma}_{n_1} = 17.5\% \pm 0.5\%$) has the smallest amount of noise with larger values for the USGS ($\hat{\sigma}_{n_2} = 18.5\% \pm 0.5\%$) and GFZ ($\hat{\sigma}_{n_3} = 20.9\% \pm 0.4\%$) catalogs. Therefore, the NDC components in the Global CMT catalog are determined most precisely.

$$\text{Cov}(n_2, n_3) > \text{Cov}(n_1, n_2) \geq 0,$$

$$\text{Cov}(n_2, n_3) > \text{Cov}(n_1, n_3) \geq 0. \quad (12)$$

Thus, the biases in the estimates for the standard deviation of the true NDC components $\hat{\sigma}_{s_{12}}$ and $\hat{\sigma}_{s_{13}}$ are higher than for the estimate based on catalogs 2 and 3, $\hat{\sigma}_{s_{23}}$. The smallest value $\hat{\sigma}_s$ obtained from our dataset through equation (10) yields the best estimate for σ_s and constitutes an upper bound for the standard deviation of the reported NDC components σ_s . We thus discard the distributions for $\hat{\sigma}_{s_{12}}$ and $\hat{\sigma}_{s_{13}}$, and calculate the standard deviation of the noise in each catalog's NDC components σ_{n_k} following equation (6) from the distribution for $\hat{\sigma}_{s_{23}}$. For the Global CMT catalog, $\sigma_{n_1} = 18.1\% \pm 0.4\%$, for the USGS catalog, $\sigma_{n_2} = 19.4\% \pm 0.4\%$, and for the GFZ catalog, $\sigma_{n_3} = 21.5\% \pm 0.4\%$ (Fig. 3b). Therefore, the NDC components are more precisely determined in the Global CMT

catalog than in any of the other 1D catalogs, likely because of partially correcting seismic waveforms for laterally varying Earth structure along the great-circle path of surface waves using a phase shift (Dziewonski *et al.*, 1984) and correcting for location in the inversion. The Global CMT catalog's standard deviation of the noise contained in its NDC components is 6.4% lower than that in the USGS catalog and 15.5% lower than that in the GFZ catalog. As a consequence of using an upper bound for the standard deviation of the true NDC components, σ_s , the estimates for the noise in each catalog's NDC components, σ_{n_k} , are a lower bound.

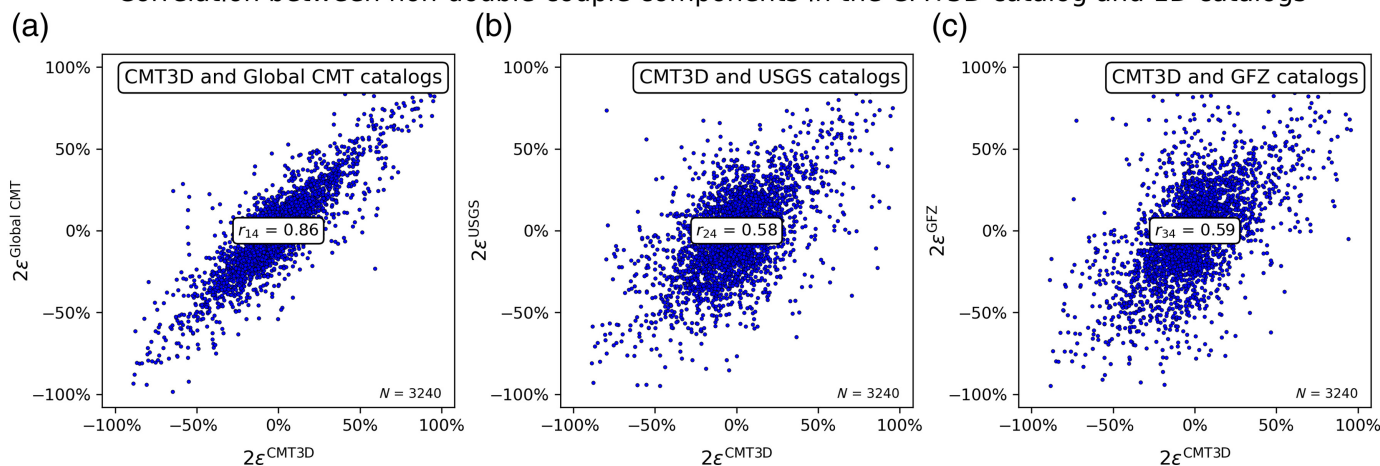
Discussion

Quantifying the noise in the NDC components through the correlation between catalogs is accurate when the inversion procedures are independent, and thus the noise in the NDC components n_{ik} is independent from the NDC components ϵ_i . As shown by the values for the standard deviation of the true NDC components, σ_s (Fig. 3a), the inversion procedures of the USGS and GFZ catalogs are not independent.

For earthquakes common to all four catalogs, the NDC components in the CMT3D catalog are very strongly correlated with those in the Global CMT catalog (Fig. 4a), reflecting the similar inversion procedure between these catalogs. The Global CMT catalog partially approximates the effects of 3D structure by shifting the seismic waveforms and adjusting the location, but uses Green's function generated for a 1D earth model in the inversion. The CMT3D moment tensor catalog, on the other hand, uses Green's functions generated for a 3D Earth model (Sawade *et al.*, 2022) for their inversion. Furthermore, the value of the correlation coefficient between the NDC components in the CMT3D and the USGS catalogs (Fig. 4b) is larger than the correlation between the CMT3D and the GFZ catalogs (Fig. 4c), similar in pattern to the correlation coefficients between the Global CMT catalog and the other 1D catalogs (Fig. 2a,b). This striking similarity of NDC components between the CMT3D and Global CMT catalogs is due to similar frequency bands used in the inversion, and a similar assignment of weights to the waveforms (Hallo and Gallovič, 2016; Sawade *et al.*, 2022). Therefore, the two catalogs invert nearly identical data for each earthquake using a nearly identical inversion procedure, leading to very similar NDC components.

The CMT3D catalog ($k = 4$) is thus not suited for the analysis of noise levels in NDC components via the correlation with other moment tensor catalogs, because it would appreciably bias the calculation of the variance of the true NDC components. However, due to the similarity of its NDC components to the Global CMT catalog and similar standard deviations ($\sigma_{d_1} = 23.7\%$, $\sigma_{d_4} = 23.8\%$) of their NDC components for earthquakes common to all four catalogs, it is reasonable to infer that the noise level in both catalogs is low and similar. The low noise level likely reflects CMT3D's use of Green's

Correlation between non-double-couple components in the CMT3D catalog and 1D catalogs



functions generated for a 3D Earth model, which reduces spurious NDC components.

When quantifying the noise in NDC components, it is useful to assess the relationship between the uncertainties in double-couple (DC) and NDC components. The similarity between the DC components of the source mechanisms in two catalogs can be quantified by the angle Φ needed to rotate the principal axes of one moment tensor into the others (Kagan, 1991). This rotation in space has values between 0° and 120° , and is 90° between pure thrust- and normal-faulting events, or for strike-slip-faulting events with opposite polarities. We correlate the rotation angles with the absolute difference between the NDC components of each moment tensor (Fig. 5).

For all pairs of catalogs, the correlation between uncertainties in DC and NDC components is weak, with coefficients of determination r^2 between 5.9% and 10.1%. This observation suggests that the mechanisms leading to uncertainties in the DC components are mostly different from those for uncertainties in NDC components.

Conclusions

NDC components contain noise stemming from the moment tensor inversion. By expressing the NDC components in moment tensor catalogs as the sum of true NDC components and random noise, we use the relationship between the correlation coefficient of NDC components in different catalogs and the standard deviation of their distribution to quantify the noise in the NDC components. The Global CMT catalog has lower noise levels than the USGS catalog, which has lower noise levels than the GFZ catalog. Due to different inversion procedures, the correlations between noise in NDC components in the Global CMT catalog with noise in the USGS and GFZ catalogs are lower than the correlations between the noise in the USGS and GFZ catalogs. Due to similarities in the inversion procedure of the CMT3D catalog and the Global CMT catalog, we cannot reliably quantify the noise

Figure 4. (a–c) Correlation between NDC components in the CMT3D catalog and the Global CMT, USGS, and GFZ catalogs. The very strong correlation with the Global CMT catalog reflects the similar inversion procedures, so the noise in both catalogs is not independent, which excludes this catalog from the quantification of its noise through the correlation with other catalogs. The color version of this figure is available only in the electronic edition.

in the CMT3D catalog using the correlation between NDC components in different catalogs. However, due to nearly identical standard deviation of the NDC components in the CMT3D catalog, we assume that the noise level is similar to the one of the Global CMT catalog.

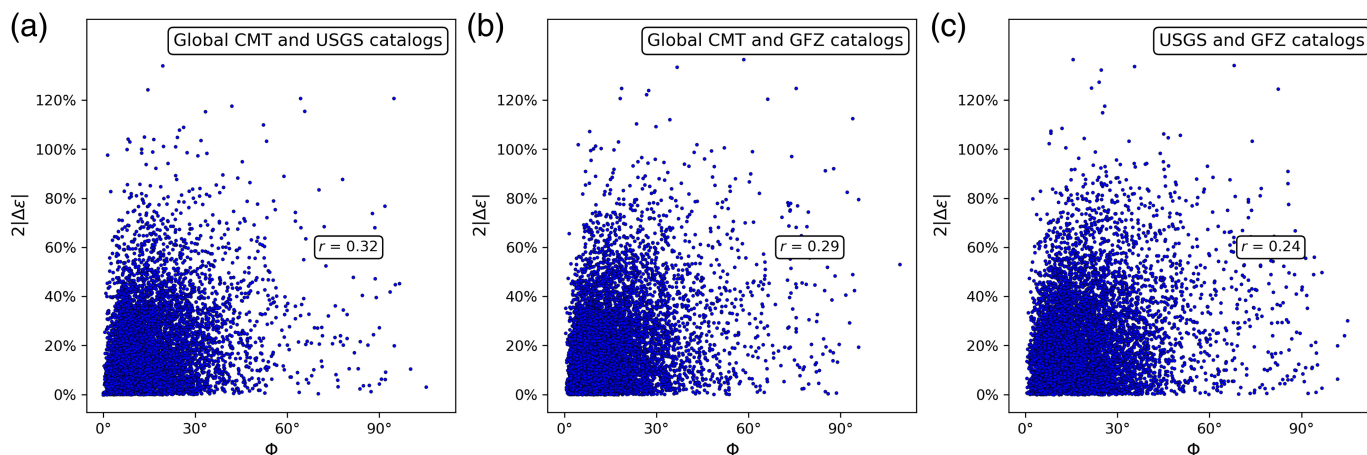
The best estimate for the standard deviation of the true NDC components is obtained as $\hat{\sigma}_s = 16.6\% \pm 0.5\%$, calculated from the correlation between the NDC components in the USGS and GFZ catalogs. Because all estimates for the noise in the NDC components, $\hat{\sigma}_{nk}$, have larger values, the estimated SNR in all catalogs, $\hat{\sigma}_s^2 / \hat{\sigma}_{nk}^2$, is smaller than 1.

Uncertainties in DC and NDC components are only weakly correlated, suggesting that uncertainties in NDC components have different origins than uncertainties in DC components. Therefore, the reliability of fault angles derived from a moment tensor is largely independent from the reliability of NDC components.

Data and Resources

The moment tensors used in this study were compiled from publicly available data sets. Global Centroid Moment Tensor (Global CMT) solutions are from <https://www.globalcmt.org> (last accessed March 2023). The U.S. Geological Survey (USGS) and German Research Centre for Geosciences (GFZ) catalogs were downloaded using the Python package ObsPy (Beyreuther *et al.*, 2010) and its International Federation of Digital Seismograph Networks webservice client (March 2023). A list of the earthquakes used in this study including their moment tensors in different catalogs is available at doi: [10.5281/zenodo.10543948](https://doi.org/10.5281/zenodo.10543948).

Correlation of differences in DC and NDC components



Declaration of Competing Interests

The authors acknowledge that there are no conflicts of interest recorded.

Acknowledgments

This research was conducted when the first author was a Japan Society for the Promotion of Science (JSPS) International Research Fellow at the Earthquake Research Institute of the University of Tokyo with Hitoshi Kawakatsu as the host researcher whom we thank for helpful discussions and suggestions for improvements of this article.

References

- Beyreuther, M., R. Barsch, L. Krischer, T. Megies, Y. Behr, and J. Wassermann (2010). ObsPy: A Python toolbox for seismology, *Seismol. Res. Lett.* **81**, no. 3, 530–533.
- Cesca, S., E. Buforn, and T. Dahm (2006). Amplitude spectra moment tensor inversion of shallow earthquakes in Spain, *Geophys. J. Int.* **166**, no. 2, 839–854.
- Cohee, B. P., and G. C. Beroza (1994). Slip distribution of the 1992 Landers earthquake and its implications for earthquake source mechanics, *Bull. Seismol. Soc. Am.* **84**, no. 3, 692–712.
- Domingues, A., S. Custodio, and S. Cesca (2013). Waveform inversion of small-to-moderate earthquakes located offshore southwest Iberia, *Geophys. J. Int.* **192**, no. 1, 248–259.
- Donner, S., M. Mustać, B. Hejrani, H. Tkalčić, and H. Igel (2020). Seismic moment tensors from synthetic rotational and translational ground motion: Green's functions in 1-D versus 3-D, *Geophys. J. Int.* **223**, no. 1, 161–179.
- Duputel, Z., L. Rivera, Y. Fukahata, and H. Kanamori (2012). Uncertainty estimations for seismic source inversions, *Seismol. Res. Lett.* **190**, no. 2, 1243–1256.
- Dziewonski, A. M., and D. L. Anderson (1981). Preliminary reference Earth model, *Phys. Earth Planet. In.* **25**, no. 4, 297–356.
- Dziewonski, A. M., J. E. Franzen, and J. H. Woodhouse (1984). Centroid-moment tensor solutions for January–March, 1984, *Phys. Earth Planet. In.* **4**, no. 34, 209–219.
- Efron, B. (1979). Bootstrap methods: Another look at the Jackknife, *Ann. Stat.* **7**, no. 1, 1–26.
- Ekström, G., M. Nettles, and A. Dziewonski (2012). The global CMT project 2004–2010: Centroid-moment tensors for 13,017 earthquakes, *Phys. Earth Planet. In.* **200–201**, 1–9.

Figure 5. (a–c) Correlation of uncertainties in double-couple (DC) and NDC components between 1D catalogs. The uncertainty in DC components is characterized by the rotation angle between principal axes. The absolute difference in NDC components is only weakly correlated to the uncertainties in DC components. The color version of this figure is available only in the electronic edition.

- Ford, S. R., D. S. Dreger, and W. R. Walter (2010). Network sensitivity solutions for regional moment-tensor inversions, *Bull. Seismol. Soc. Am.* **100**, no. 5A, 1962–1970.
- Giardini, D. (1984). Systematic analysis of deep seismicity: 200 centroid-moment tensor solutions for earthquakes between 1977 and 1980, *Geophys. J. Int.* **77**, no. 3, 883–914.
- Gudmundsson, M. T., K. Jónsdóttir, A. Hooper, E. P. Holohan, S. A. Halldórsson, B. G. Ófeigsson, S. Cesca, K. S. Vogfjörð, F. Sigmundsson, T. Högnadóttir, *et al.* (2016). Gradual caldera collapse at Bárðarbunga volcano, Iceland, regulated by lateral magma outflow, *Science* **353**, no. 6296, doi: [10.1126/science.aaf898](https://doi.org/10.1126/science.aaf898).
- Hallo, M., and F. Gallovič (2016). Fast and cheap approximation of Green function uncertainty for waveform-based earthquake source inversions, *Geophys. J. Int.* **207**, no. 2, 1012–1029.
- Hamling, I. J., S. Hreinsdóttir, K. Clark, J. Elliott, C. Liang, E. Fielding, N. Litchfield, P. Villamor, L. Wallace, T. J. Wright, *et al.* (2017). Complex multifault rupture during the M_w 7.8 Kaikōura earthquake, New Zealand, *Science* **356**, no. 6334, doi: [10.1126/science.aam7194](https://doi.org/10.1126/science.aam7194).
- Hayes, G. P., R. W. Briggs, A. Sladen, E. J. Fielding, C. Prentice, K. Hudnut, P. Mann, F. W. Taylor, A. J. Crone, R. Gold, *et al.* (2010). Complex rupture during the 12 January 2010 Haiti earthquake, *Nature Geosci.* **3**, no. 11, 800–805.
- Hayes, G. P., L. Rivera, and H. Kanamori (2009). Source inversion of the W-Phase: Real-time implementation and extension to low magnitudes, *Seismol. Res. Lett.* **80**, no. 5, 817–822.
- Hejrani, B., H. Tkalčić, and A. Fichtner (2017). Centroid moment tensor catalogue using a 3-D continental scale Earth model: Application to earthquakes in Papua New Guinea and the Solomon Islands, *J. Geophys. Res.* **122**, no. 7, 5517–5543.
- Hingee, M., H. Tkalčić, A. Fichtner, and M. Sambridge (2011). Seismic moment tensor inversion using a 3-D structural model:

- Applications for the Australian region, *Geophys. J. Int.* **184**, no. 2, 949–964.
- Hjörleifsdóttir, V., and G. Ekström (2010). Effects of three-dimensional Earth structure on CMT earthquake parameters, *Phys. Earth Planet. In.* **179**, nos. 3/4, 178–190.
- Jechumtálová, Z., and J. Šílený (2001). Point-source parameters from noisy waveforms: Error estimate by Monte-Carlo simulation, *Pure Appl. Geophys.* **158**, no. 9, 1639–1654.
- Kagan, Y. Y. (1991). 3-D rotation of double-couple earthquake sources, *Geophys. J. Int.* **106**, no. 3, 709–716.
- Kanamori, H., and J. W. Given (1982). Analysis of long-period seismic waves excited by the May 18, 1980, eruption of Mount St. Helens—A terrestrial monopole? *J. Geophys. Res.* **87**, no. B7, 5422–5432.
- Kawakatsu, H. (1991). Enigma of earthquakes at ridge-transform-fault plate boundaries distribution of non-double-couple parameter of Harvard CMT solutions, *Geophys. Res. Lett.* **18**, no. 6, 1103–1106.
- Minson, S. E., M. Simons, and J. L. Beck (2013). Bayesian inversion for finite fault earthquake source models I-Theory and algorithm, *Geophys. J. Int.* **194**, no. 3, 1701–1726.
- Minson, S. E., M. Simons, J. L. Beck, F. Ortega, J. Jiang, S. E. Owen, A. W. Moore, A. Inbal, and A. Sladen (2014). Bayesian inversion for finite fault earthquake source models I-Theory and algorithm, *Geophys. J. Int.* **198**, no. 2, 922–940.
- Nettles, M., and G. Ekström (1998). Faulting mechanism of anomalous earthquakes near Bárðarbunga volcano, Iceland, *J. Geophys. Res.* **103**, no. B8, 17973–17983.
- Pang, G., K. D. Koper, M. Mesimeri, K. L. Pankow, B. Baker, J. Farrell, J. Holt, J. M. Hale, P. Roberson, R. Burlacu, *et al.* (2020). Seismic analysis of the 2020 Magna, Utah, earthquake sequence: Evidence for a listric Wasatch fault, *Geophys. Res. Lett.* **47**, no. 18, doi: [10.1029/2020GL089798](https://doi.org/10.1029/2020GL089798).
- Phạm, T. S., and H. Tkalčić (2021). Accounting for theory errors with empirical Bayesian noise models in nonlinear centroid moment tensor estimation, *J. Geophys. Res.* **126**, no. 11, doi: [10.1093/gji/ggab034](https://doi.org/10.1093/gji/ggab034).
- Rodríguez-Cardozo, F., V. Hjörleifsdóttir, K. Jónsdóttir, A. Iglesias, S. I. Franco, H. Geirsson, N. Trujillo-Castrillón, and M. Hensch (2021). The 2014–2015 complex collapse of the Bárðarbunga caldera, Iceland, revealed by seismic moment tensors, *J. Volcanol. Geotherm. Res.* **416**, 107275, doi: [10.1016/j.jvolgeores.2021.107275](https://doi.org/10.1016/j.jvolgeores.2021.107275).
- Rösler, B., and S. Stein (2022). Consistency of non-double-couple components of seismic moment tensors with earthquake magnitude and mechanism, *Seismol. Res. Lett.* **93**, no. 3, 1510–1523.
- Rösler, B., S. Stein, and S. E. Hough (2022). On the documentation, independence, and stability of widely used seismological data products, *Front. Earth Sci.* **10**, 988098, doi: [10.3389/feart.2022.988098](https://doi.org/10.3389/feart.2022.988098).
- Rösler, B., S. Stein, and B. D. Spencer (2021). Uncertainties in seismic moment tensors inferred from differences between global catalogs, *Seismol. Res. Lett.* **92**, no. 6, 3698–3711.
- Rößler, D., F. Krüger, and G. Rumpker (2007). Retrieval of moment tensors due to dislocation point sources in anisotropic media using standard techniques, *Geophys. J. Int.* **169**, no. 1, 136–148.
- Rösler, B., S. Stein, and B. D. Spencer (2023). When are non-double-couple components of seismic moment tensors reliable? *Seismica* **2**, no. 1, doi: [10.26443/seismica.v2i1.241](https://doi.org/10.26443/seismica.v2i1.241).
- Ross, A., G. R. Foulger, and B. R. Julian (1996). Non-double-couple earthquake mechanisms at the Geysers geothermal area, California, *Geophys. Res. Lett.* **23**, no. 8, 877–880.
- Ruhl, C. J., E. A. Morton, J. M. Bormann, R. Hatch-Ibarra, G. Ichinose, and K. D. Smith (2021). Complex fault geometry of the 2020 M_{ww} 6.5 Monte Cristo Range, Nevada, earthquake sequence, *Seismol. Res. Lett.* **92**, no. 3, 1876–1890.
- Sandanbata, O., H. Kanamori, L. Rivera, Z. Zhan, S. Watada, and K. Satake (2021). Moment tensors of ring-faulting at active volcanoes: Insights into vertical-CLVD earthquakes at the Sierra Negra caldera, Galápagos Islands, *J. Geophys. Res.* **126**, no. 6, doi: [10.1029/2021JB021693](https://doi.org/10.1029/2021JB021693).
- Sawade, L., S. Beller, W. Lei, and J. Tromp (2022). Global centroid moment tensor solutions in a heterogeneous earth: The CMT3D catalogue, *Geophys. J. Int.* **231**, no. 3, 1727–1738.
- Scognamiglio, L., E. Tinti, E. Casarotti, S. Pucci, F. Villani, M. Cocco, F. Magnoni, A. Michelini, and D. Dreger (2018). Complex fault geometry and rupture dynamics of the M_w 6.5, 30 October 2016, central Italy earthquake, *J. Geophys. Res.* **123**, no. 4, 2943–2964.
- Shuler, A., G. Ekström, and M. Nettles (2013). Physical mechanisms for vertical-CLVD earthquakes at active volcanoes, *J. Geophys. Res.* **118**, no. 4, 1569–1586.
- Shuler, A., M. Nettles, and G. Ekström (2013). Global observation of vertical-CLVD earthquakes at active volcanoes, *J. Geophys. Res.* **118**, no. 1, 138–164.
- Šílený, J. (2004). Regional moment tensor uncertainty due to mismodeling of the crust, *Tectonophysics* **383**, nos. 3/4, 133–147.
- Šílený, J., P. Campus, and G. F. Panza (1996). Seismic moment tensor resolution by waveform inversion of a few local noisy records—I. Synthetic tests, *Geophys. J. Int.* **126**, no. 3, 605–619.
- Silver, P. G., and T. H. Jordan (1982). Optimal estimation of scalar seismic moment, *Geophys. J. Int.* **70**, no. 3, 755–787.
- Vasyura-Bathke, H., J. Dettmer, R. Dutta, P. M. Mai, and S. Jonsson (2021). Accounting for theory errors with empirical Bayesian noise models in nonlinear centroid moment tensor estimation, *Geophys. J. Int.* **225**, no. 2, 1412–1431.
- Vera Rodríguez, I., Y. J. Gu, and M. D. Sacchi (2011). Resolution of seismic-moment tensor inversions from a single array of receivers, *Bull. Seismol. Soc. Am.* **101**, no. 6, 2634–2642.
- Wald, D. J., and T. H. Heaton (1994). Spatial and temporal distribution of slip for the 1992 Landers, California, earthquake, *Bull. Seismol. Soc. Am.* **84**, no. 3, 668–691.
- Yang, J., H. Zhu, T. Lay, Y. Niu, L. Ye, Z. Lu, B. Luo, H. Kanamori, J. Huang, and Z. Li (2021). Multi-fault opposing-dip strike-slip and normal-fault rupture during the 2020 M_w 6.5 Stanley, Idaho earthquake, *Geophys. Res. Lett.* **48**, no. 10, doi: [10.1029/2021GL092510](https://doi.org/10.1029/2021GL092510).

Manuscript received 6 November 2023
Published online 6 March 2024